TYCHO EJECTA DEPOSITS NEAR THE BALLISTIC ANTIPODE: NEW MODELING METHODS.

J. B. Adler[1], E. Asphaug[2], M. S. Robinson[1], A. Winhold[1], T. M. Davison[3], N. Artemieva[4] [1]Arizona State University School of Earth and Space Exploration, Tempe, AZ, USA; [2]Lunar and Planetary Lab, University of Arizona, Tucson, AZ, USA. [3]Dept. of Earth Science & Engineering, Imperial College, London, UK. [4]Planetary Science Institute, Tucson, AZ. (Jacob.B.Adler@asu.edu)

Introduction: This work investigates the distribution of Tycho ballistic ejecta across the Moon, including its antipode. Using a 3D hydrocode and precise orbital propagation software, we compute the distribution of ejecta particles from the Tycho impact. This simulation addresses how the highland melt ponds and anomalous rock abundance may have formed as a result of antipodal ballistic focusing from the Tycho impact event, ~108 Ma ago [1-3]. Our new model improves upon previous work [3-7] by incorporating effects from high-resolution gravity data, topography data, and tidal forces on the ballistic ejecta from a high-resolution 3D impact simulation of Tycho.

We will test how topographic shadowing, lunar rotation rate, and gravity model resolution factor in to the ballistic model. Second order influences such as tidal forces from the Earth could also have a significant effect on ejecta flight paths. Lunar rotation rate and distance from Earth have changed throughout the Moon's history, thus we have varied these parameters to measure the antipodal ballistic distribution of impacts earlier in the Moon's history.

Background: Terrains antipodal to large impacts are believed to be formed by the focusing of seismic waves traveling through the lunar interior [8] or by emplacement of far-flung ejecta [9]. While the seismic process has been examined and characterized [10,11], the degree of focusing and offset for the ballistic ejecta case remains less understood. Nonetheless, ballistic emplacement of material near the antipodes of impacts is consistently among the top hypotheses for the source of several melt pond fields [1,2,12] and as a formation mechanism for lunar magnetic swirls [13]. Contemporary lunar studies often invoke an antipodal emplacement mechanism to reconcile anomalous landforms, but without a physical model to recreate and characterize this process, these hypotheses were difficult to test [1,14].

In this work, we create a model of antipodal ejecta emplacement to answer the following questions: How much is the ballistic antipode offset from the geometric antipode? Do high-resolution variations in gravity, or tidal forces significantly affect the ballistic distribution? We test the antipodal impact source hypothesis for the highland melt pond case.

Other Models: Foundational work describing ballistic trajectories reaching the antipode can be found in [15], which provides equations for focus point offset due to the Coriolis force. Preliminary spectroscopic work at the highland ponds is presented in [5,16]. Extensive hydrocode antipodal modeling for this precise Tycho test case is described in [4,9]. Their results show an increased ejecta deposit at the antipode which is most noticeable for large impacts. Their results show deposits as thick as 1 km at the antipode of a 200 km diameter projectile impact, and deposits as thick as 50 m at the antipode of a 50 km diameter projectile impact. Additionally, preliminary results from a ballistic ray-tracing model employed by [3,6,7] account for the expected offset and bi-directionality of highland melt pond deposits [2]. Their model incorporated lunar rotation and topographic shadowing [3]. They proposed that frictional heating of repeated impacts was sufficient to re-melt this distal ejecta and explain the pond morphology.

Methods: We use two different hydrocode models, SOVA [17] and iSALE 3D [18,19], for increased confidence of ejecta distribution and for benchmarking the two models. We used 3D hydrocodes since the Tycho impactor is thought to have low angle (15-30° above the horizon) and thus ejecta was highly directionalized [20]. The projectile impacted at 20 km/s at 30° from the southwestern horizon. Results of the 3D impact simulation are recorded as ejecta velocity vectors at a height of 0.5 km above the pre-impact surface. The origin material and state of tracers is also recorded (i.e. solid target, molten target, solid projectile, molten projectile, vapor projectile). We ignore ejecta above the escape velocity (~2.4 km/s) and those categorized as vapor, since both result in non-ballistic orbits.

We utilized the STK [21] software (11.4.1) to propagate ejecta through ballistic trajectories (Fig. 1), and to vary the lunar gravity model, rotation rate, tidal force, and topography. STK is a high-fidelity orbital propagator that has been used for orbit designs for missions including LRO. The software offers control of many of

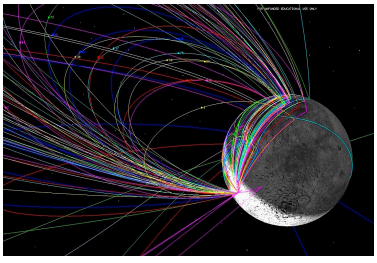

Fig. 1. Ballistic trajectories of a subset of 100 Tycho ejecta tracers in STK.

the methods of orbital propagation, including the gravity field of the Moon to degree and order 600, as well as the gravitational influence of the Earth and Sun. (The Moon was about 1 Earth radius closer to Earth when Tycho formed, but this should amount to little difference in the tidal forces on ballistic ejecta.) The software provides control of the planets' ephemerides, which is a powerful tool for impact ejecta modeling earlier in the Moon's history. To automate each run and produce ejecta distribution maps we used the STK handle functionality within MATLAB (2015a) [22] to repeatedly invoke STK in the background (skipping graphical displays and animation) for each tracer. We plot preliminary results from our pilot study in Fig. 2.

Preliminary Results: We propagated ~600 ejecta particles from their predicted origins to their ballistic landing points from a small azimuthal wedge of ejecta velocities (0-110° N of E; 2.0-2.4 km/s) roughly aligned with the proposed downfield projectile direction [20]. Our results show successful implementation of this workflow, but interpretation of the pilot study map should be cautioned due to only a small fraction of ejecta being tested.

The distribution map shows a concentration of ejecta centered around 70°E, 15°N (including the Apollo 17 landing site). Secondary craters from Tycho are known in this area, and Fig. 3 shows units inferred to be Tycho ejecta rays [23]. Tycho crater's young age makes it a key lunar calibration point, and radiometric dating of returned samples from Apollo 17 in this region have been used to infer Tycho's age [23-27].

The model currently shows no ejecta between the nearside area and the antipode. This shadowed area (see Fig. 2; area centered at 120°E, 40°N) may be due to the limited number of particle tracers that have been evolved, rather than a true shadowing effect. Our next model will propagate more ejecta particles to test these results.

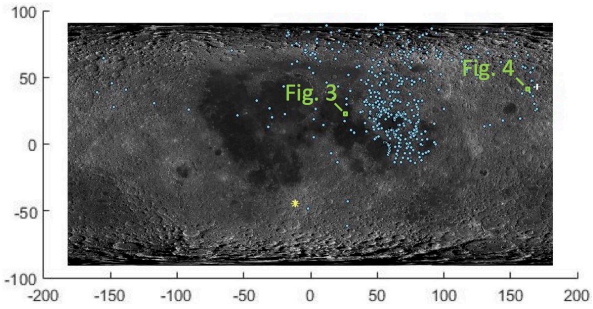

Fig. 2. Tycho ejecta distribution from a subset of 600 particles. Tycho crater and geometric antipode shown as yellow star and white cross. Ejecta landing locations for a small azimuthal wedge of 3D SOVA hydrocode output in the velocity range 2.0–2.4 km/s shown in blue.

There are landing locations near the Tycho antipode, coincident with where the highland melt ponds [1] and Diviner rock abundance anomaly occur [2]. These ponds (e.g., Fig. 4) are smooth, flat, lightly-crated deposits in topographic depressions, which appear to have flowed or settled to their position. They are presumed to be ballistically emplaced impact melt (volcanism and basin ejecta were ruled out), but candidate source craters could not be definitively tied to these deposits [1]. Our results show it is possible for high-velocity ejecta from Tycho to reach this region near its antipode.

Conclusion: We implemented a novel workflow for Tycho high-velocity ejecta propagation. This model incorporates a 3D impact hydrocode (i.e., SOVA, iSALE-3D) and precise orbital propagation software (STK). Preliminary results confirm that Tycho ejecta reaches the antipode, and appears to be concentrated there. As expected, ejecta lands in larger quantities downrange from the crater. Ongoing work using the full crater ejecta distribution, to be presented, will be used to assess the degree to which this is statistically significant.

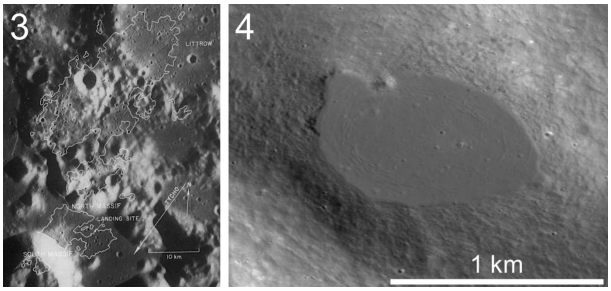

Fig. 3. Secondary craters on the Tycho-facing side of several highland massifs near the Apollo 17 landing site as shown in Figure 7 from *Lucchitta, 1977*. Fig. 4. An example melt pond near the Tycho antipode as imaged by the LROC NAC.

References: [1] Robinson et al., (2016) *Icarus*, *273*, 121-134. [2] Bandfield et al., (2017) *Icarus*, *283*, 282-299. [3] Paige et al., (2018) *LPSC*, #2757. [4] Artemieva (2013), *LPSC*, #1413. [5] Paige et al., (2018) *EPSC*, #603. [6] Jögi and Paige (2014) *LPSC*, #2574. [7] Jögi and Paige (2015) *LPSC*, #2779. [8] Schultz and Gault (1975) *LPSC*, 2845-2862. [9] Hood and Artemieva, (2008) *Icarus*, *193*, 485-502. [10] Retailleau et al., (2014) *Geophysical J. Int.*, *199*, 2, 1030-1042. [11] Rial (1978) *Geophysical J. Int.*, *55*, 3, 737-743. [12] Williams et al., (2015) *LPSC*, #2738. [13] Hood et al., (2013), *JGR:Planets*, *118*, 1265-1284. [14] Greenhagen et al., (2013) *LPSC*, #2987. [15] Dobrovolskis (1981) *Icarus*, *47*, 203-219. [16] Curren et al., (2018) *EPSC*, #748. [17] Shuvalov V. (1999) *Shock Waves*, *9*, 381-390 [18] Amsden and Ruppel (1981) *Report LA-8905*, LANL. 151 p. [19] Elbeshausen et al., (2009) *Icarus*, *204*, 716-731. [20] Krüger et al., (2013) *LPSC*, #2152 [21] Analytical Graphics, Inc., STK, http://www.agi.com [22] The Mathworks, Inc., Natick, Massachusetts. MATLAB (R2015a). [23] Lucchitta (1977) *Icarus* 30, 80-96. [24] Hiesinger et al., (2012) *JGR*, *117*, E00H10. [25] Arvidson et al., (1976) *LPSC*, 2817-2832. [26] Drozd et al., (1977) *LPSC*, 3027-3043. [27] Guinness and Arvidson (1977) *LPSC*, 3475-3494.